Precise control of interface anisotropy during deposition of Co/Pd multilayers

C. W. Barton, T. J. A. Slater, R. M. Rowan-Robinson, S. J. Haigh, D. Atkinson, and T. Thomson

Citation: Journal of Applied Physics **116**, 203903 (2014); doi: 10.1063/1.4902826
View online: https://doi.org/10.1063/1.4902826
View Table of Contents: http://aip.scitation.org/toc/jap/116/20
Published by the American Institute of Physics

Precise control of interface anisotropy during deposition of Co/Pd multilayers

C. W. Barton,[1,a)] T. J. A. Slater,[2] R. M. Rowan-Robinson,[3] S. J. Haigh,[2] D. Atkinson,[3] and T. Thomson[1]
[1]*School of Computer Science, The University of Manchester, Oxford Rd, Manchester M13 9PL, United Kingdom*
[2]*School of Materials, The University of Manchester, Oxford Rd, Manchester M13 9PL, United Kingdom*
[3]*Department of Physics, Durham University, South Rd, Durham DH1 3LE, United Kingdom*

(Received 4 July 2014; accepted 12 November 2014; published online 26 November 2014)

We demonstrate the control of perpendicular magnetic anisotropy (PMA) in multilayer films without modification of either the microstructure or saturation magnetization by tuning the Ar^+ ion energy using remote plasma sputtering. We show that for $[Co/Pd]_8$ multilayer films, increasing the Ar^+ ion energy results in a strong decrease in PMA through an increase in interfacial roughness determined by X-ray reflectivity measurements. X-ray diffraction and transmission electron microscope image data show that the microstructure is independent of Ar^+ energy. This opens a different approach to the *in-situ* deposition of graded exchange springs and for control of the polarizing layer in hybrid spin transfer torque devices. © *2014 AIP Publishing LLC*.
[http://dx.doi.org/10.1063/1.4902826]

INTRODUCTION

Co/Pd multilayer films exhibit high perpendicular magnetic anisotropy (PMA)[1] and high exchange coupling. This makes them attractive candidates for future technologies, such as bit patterned media (BPM) for magnetic recording beyond 1 Tbit/in^2 and as component layers in spin transfer torque (STT) based devices.[2,3]

In the regime where individual layers approach monolayer thicknesses, the magnetic properties of Co/Pd multilayers are controlled by the layer thickness,[4] number of repeats,[5] crystallographic texturing,[6] grain size, and interface quality. The choice of seed layer(s) affects the texturing, microstructure, and interfaces.[7] For example, higher anisotropy materials have been created using enhanced seed layers, e.g., Ta/Pd. Deposition conditions are equally important since it is well known that sputtering gas pressure can be used to refine grain size in thin films.[8]

Since the first reports on Co/Pd[1] (or Co/Pt (Ref. 9)) perpendicular anisotropy multilayer films, it has been understood that varying the thickness of the Co layer provides a sensitive method of tuning the anisotropy.[4] However, changing the Co thickness also changes the saturation magnetisation and hence the two parameters cannot be controlled independently. Recently, Hauet *et al.*[10] and Maziewski *et al.*[11] showed that control of PMA can be achieved by *ex-situ* ion irradiation, where chemical intermixing at the interface was responsible for a reduction in uniaxial anisotropy and consequently a decrease in the nucleation field. Additional control of the interface properties was demonstrated by Pierce *et al.*,[12] where changing the working gas pressure was found to increase interface roughness reducing the perpendicular anisotropy. Increasing the pressure was shown to cause chemical segregation and grain formation which acts to reduce grain-grain exchange coupling a property undesirable for application in BPM and STT devices.

In this work, we report an *in-situ* method of tuning the PMA of (111) textured $[Co/Pd]_8$ multilayers, by changing the acceleration energy of the incident Ar^+ ions using a sputter system with a remotely generated plasma source.[13] This has the advantage of decoupling the plasma properties from the sputtering process which is not possible using conventional dc or rf magnetron sputtering.

EXPERIMENTAL METHODS

Remote plasma sputtering is undertaken using a PlasmaQuest HiTUS system attached to a Lesker vacuum chamber. The plasma is generated using a helicon resonator combined with a solenoid field, located outside the main chamber. The essential features of this class of remote plasma sputtering system have been described by Vopsaroiu *et al.*[14] We deposit multilayers with a structure similar to many of those reported in the literature.[4,10] The nominal structure was Ta(30 Å)/Pd(60 Å)/[Co(3 Å)/Pd(9 Å)]$_8$/Pd(11 Å), deposited on SiO_2/Si substrates. The working pressure of Ar gas was 3×10^{-3} mbar, where the base pressure prior to deposition was $<9 \times 10^{-9}$ mbar. A series of films were deposited at four different Ar^+ ion energies ranging from 200 eV to 1 keV, where the seed layer deposition energy was matched to the multilayer deposition energy. Additionally, a separate series were fabricated to investigate the effect of keeping the seed layer energy fixed at 200 eV. X-ray diffraction (XRD) was performed using a Phillips X'pert Pro diffractometer with CuK_α radiation in order to investigate the crystallographic structure. X-ray reflectivity (XRR) was performed with a Bede D1 diffractometer with CuK_α radiation to investigate the out-of-plane interface width. The magnetic properties were studied by vibrating sample magnetometry (VSM) using a MicroSense model 10 vector VSM. The

a)Electronic mail: craig.barton@manchester.ac.uk

microstructure and polycrystalline grain sizes were investigated by transmission electron microscope (TEM) imaging using a Philips CM20 microscope operating at 200 kV.

RESULTS AND DISCUSSION

Fig. 1(a) shows in-plane hysteresis loops as a function of Ar^+ energy for the four different Ar^+ ion energies. These data clearly show that changing the deposition conditions results in a dramatic change in magnetic properties. The loops change from those characteristic of a hard-axis measurement for the 200 eV sample to an easy axis measurement for the 1 keV sample. In the case of a hard-axis loop, the anisotropy field H_k can be determined using the second and fourth quadrants following the methodology used by Thomson *et al.*[15] The anisotropy field is then used to calculate the uniaxial anisotropy (K_u) and magnetocrystalline anisotropy (K_1) through the following equation:

$$H_k = 2K_u/M_s, \tag{1}$$

where M_s is the saturation magnetisation, $K_u = K_1 + K_s$ with shape anisotropy (K_s) given by $K_s = 2\pi M_s^2$ which is the normal thin film assumption, appropriate for highly exchange coupled, metallically continuous films.

Fig. 1(b) shows the values of K_u and K_1 obtained from the measured value of H_k together with the saturation magnetisation, which remains constant at $\sim 500 \pm 30$ emu cm^{-3} (inset). The perpendicular magnetocrystalline anisotropy reduces monotonically with increasing Ar^+ ion energy and for the 1 keV sample, the effect of the in-plane shape anisotropy overcomes the perpendicular magnetocrystalline anisotropy and the magnetization lies in the plane of the film. Figure 1 also shows that fixing the seed layer deposition bias voltage at 200 eV produces a similar functional form of K_u

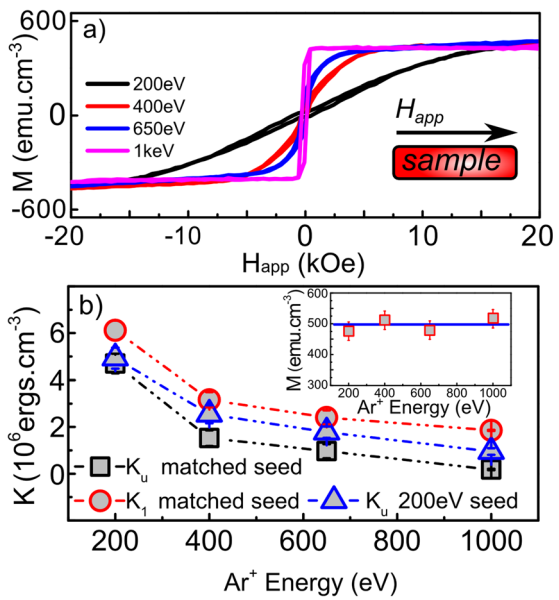

FIG. 1. [(a) and (b)] VSM measurements of $[Co/Pd]_8$ multilayers deposited at Ar ion energies of 200 eV, 400 eV, 650 eV, and 1 keV: (a) shows the in-plane hysteresis loops and (b) shows how K_u and K_1 vary as the Ar^+ ion energy is increased (black squares and red circles, respectively) and K_u for the samples deposited onto a 200 eV seed, inset shows M_s.

with the Ar^+ ion energy. The PMA of Co/Pd multilayers is understood to predominantly arise from the reduced symmetry at the site of the Co atom[16,17] and magnetoelastic[18] effects for Co layer thickness of $t_{Co} < 8$ Å. All subsequent measurements were performed on the sample series, where the seed layers were deposited under the same conditions as the magnetic multilayer.

In order to unambiguously identify the origins of the change in anisotropy with Ar^+ energy, we investigated the structural properties of the multilayers. All the samples were grown on Ta/Pd seed layers which were also deposited as a function of Ar^+ ion energy. Fig. 2(a) shows XRD results for the Ta/Pd seed layers before deposition of the [Co/Pd] multilayer, demonstrating these have an out-of-plane Pd (111) texture with $d_{(111)} = 2.24$ Å and that this does not change with Ar^+ ion energy. Fig. 2(b) shows XRD data acquired for the full-film structure with the Co/Pd (222) reflection shown in the inset, Fig. 2(c). Fig. 2(d) summaries these XRD results and demonstrates an out-of-plane Co/Pd texture with a mean d-spacing $d_{(111)} = 2.22$ Å consistent with a coherently strained multilayer system.[6] Large angle ω-rocking curves, Fig. 2(e), performed at the Pd(111) peak show that the full width half max (FWHM) increases slightly from $\sim 6.4°$ to $7.1°$ as the Ar^+ ion energy is increased. The FWHM values are plotted, inset Fig. 2(e). All peak analyses of the

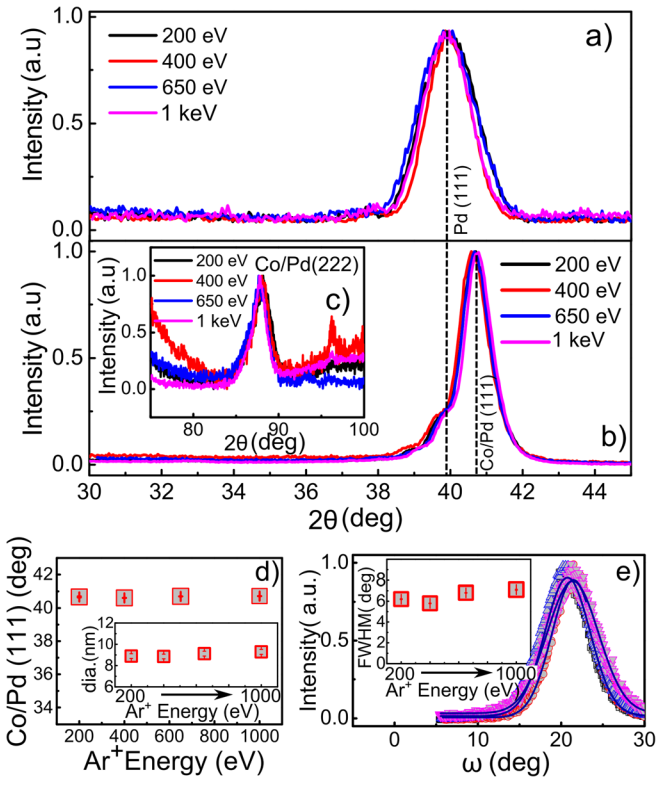

FIG. 2. [(a)–(e)] XRD analysis of the $[Co/Pd]_8$ multilayer deposited at Ar ion energies of 200 eV, 400 eV, 650 eV, and 1 keV taken using CuK_α radiation: (a) is large angle $\theta - 2\theta$ diffraction scans of the Ta/Pd seed layers (SiO_2 peaks subtracted), while (b) shows the $\theta - 2\theta$ scans of full-film structure; inset (c) shows the second order Bragg diffraction condition n = 2; (d) Bragg angles for the full-film structure as a function of Ar ion energy (inset shows the grain diameter analysis); (e) ω-rocking curves (blue line is the Pearson VII fit), where inset shows the FWHM values (squares) as a function of the Ar^+ ion energy, errors are within symbols.

XRD data were performed using nonlinear least square fitting of a Pearson VII function,[19] where the peak line shape is allowed to vary between purely Lorentzian and purely Gaussian to account for strain and crystallite size. The width of the XRD diffraction peak provides an indication of the grain size and is frequently analysed via the Scherrer equation.[20] The results of this analysis give a mean grain diameter of ~9 nm that is independent of Ar^+ ion energy, within measurement accuracy (±0.5 nm) as shown in the inset of Fig. 2(d). These XRD data demonstrate that increasing the Ar^+ ion energy introduces no change in the out-of-plane crystallographic orientation or grain size of the Co/Pd multilayers.

The layer structure of the multilayers was investigated using XRR to determine the out-of-plane scattering vector, q_z, and hence the total interface width, σ. The detector angle was scanned in the range $0° < 2\theta < 9°$ and the results are shown in Fig. 3(a). The experimental data were fitted using the Bede REFS software package,[21] which employs the Parrat recursive formulism[22] to find the best fit to the data.[23] The apparent variation in the spectra is thought to mainly arise from the slight variation in the seed layer thickness. The inset, Fig. 3(b), shows a summary of the weighted average out-of-plane interface width for the full-film structure σ_{FS} (including the adhesion, seed, magnetic, and capping layers) and the bilayer only σ_{BL} (magnetic bilayer only), Fig. 3(c), which were obtained from the fitting procedure. These data demonstrate a clear increase from 3.0 Å to 5.5 Å

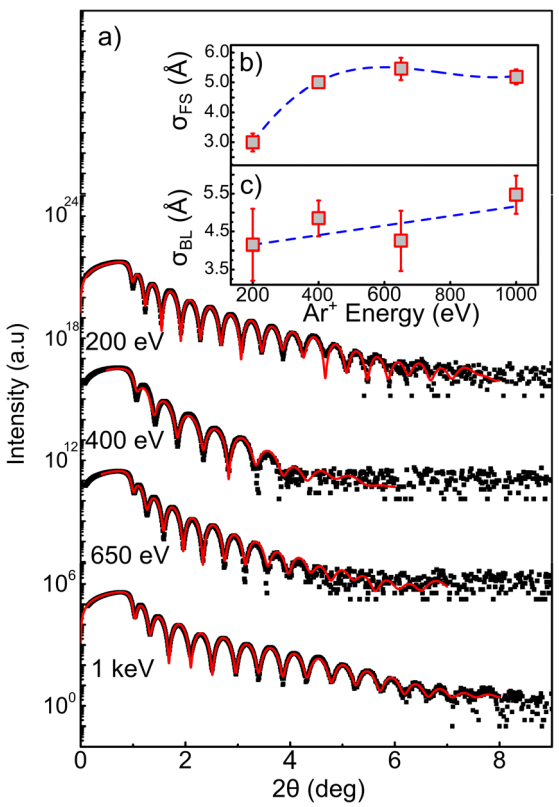

FIG. 3. [(a)–(c)] XRR coupled $\theta - 2\theta$ specular curves of the [Co/Pd] multilayer full-film structures showing the experimental data (black squares) and the best-fit (red line); the insets (b) and (c) show the weighted average of the out-of-plane interface width for full-film structure σ_{FS} and bilayer only σ_{BL} as a function of the Ar^+ ion energy, dashed blue lines are a guide to the eye.

in the out-of-plane interface width, a combined contribution from interface roughness, and compositional interface grading. However in these films, it is expected that interface roughness on the order seen here would not have such a significant effect on the measured anisotropy. More likely, it is a change in the atomic coordination number at the interface due to interfacial mixing of the Co and Pd atoms. That is, the higher the energy used during the deposition, the larger the disruption to the interfacial ordering at the atomic site of Co. This reduced symmetry breaking at the interface leads directly to a reduced interface anisotropy contribution to K_u lowering PMA.

TEM allows accurate investigation of local grain size but requires samples to be sufficiently thin that they are electron transparent. Therefore, sister samples were produced by depositing the multilayer films onto 50 nm SiN_x membranes to investigate possible changes in microstructure. Fig. 4(a) shows an example electron diffraction pattern for the sample deposited at 650 eV and includes scattering contributions from crystallographic planes other than the (111) observed in the XRD data, Figs. 2(a) and 2(b). This is emphasised by the profile plot (white-line) obtained from the section indicated by the dotted line and shows the indexed peaks attributed to the (111), (022), (113), (122), and (224) diffracting planes of Co/Pd. Fig. 4(b) shows an example of a dark field TEM image for this deposition energy with the corresponding bright field image shown inset in Fig. 4(b). Grain size analysis was performed by manual measurement of the grain size for ≈400 grains contained in multiple dark field images. The mean grain diameter $\bar{D}_\mu$ as a function of Ar^+ ion energy is summarised in Fig. 4(c), and demonstrates that $\bar{D}_\mu$ remains constant with a value of approximately 6 nm within ± one standard deviation (2 nm). The distribution of grain sizes shows the expected log-normal probability density function,[14] inset Fig. 4(c), which is determined by the grain growth and the nucleation rate.[24] The grain sizes obtained by

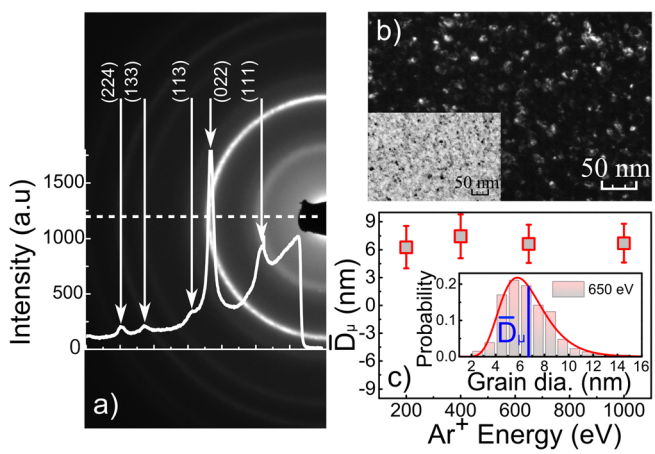

FIG. 4. [(a)–(d)] TEM analysis of the multilayer Co/Pd thin film samples deposited onto SiN_x membranes: (a) indexed electron diffraction pattern with superimposed intensity profile (white-line) corresponding to the dotted line; (b) is the dark field micrograph for the sample deposited at 650 eV (inset is the corresponding bright field micrograph); (c) is the grain size measured from dark field TEM images as a function of Ar^+ ion energy, inset shows an example grain size distribution for the sample deposited at 650 eV, where the blue line shows $\bar{D}_\mu$.

TEM and XRD are in very good agreement and crucially both measurements show that grain size remains, within error, constant for samples deposited at different Ar^+ energies. This lack of change in the crystallographic orientation or granularity strongly suggests that the reduction in K_u is attributed solely to changes in the interface quality.[25]

The effect of Ar^+ ion energy on magnetization reversal has also been investigated. Hysteresis loops, where the field was applied perpendicular to the plane of the sample, show that the nucleation field reduces as the Ar^+ ion energy is increased, Fig. 5(a). The 1 keV sample has lost its PMA, as described earlier. Since the microstructure, saturation magnetization, and thickness of the films do not change, it is possible to make the assumption that the nucleation field scales with anisotropy. This ability to vary one parameter at a time is a key advantage of our approach. The normalised (by area) switching field distribution (SFD) $\frac{dM}{dH_{app}}$, is shown in Fig. 5(b), for the 200 eV, 400 eV, and 650 eV multilayer films. These data show that a broad tail in the SFD develops as the Ar^+ ion energy is increased and this tail is attributed to the domain-wall pinning/annihilation.[26] The increase in SFD tail occurs at the same time as a reduction of the nucleation field and can be understood in terms of the Mansuripur two-coercivity model.[27]

The two-coercivity model highlights two extreme cases of magnetisation reversal in thin films with PMA: (i) the energy barrier due to nucleation is greater than that of domain-wall pinning which leads to sharp/square hysteresis loops; and (ii) the energy barrier due to nucleation is less than that of domain-wall pinning leading to a rounding of the hysteresis loop as domain-wall pinning becomes more important in controlling the reversal process. This effect can be observed in our films as broadening in the tail of the SFD due to domain-wall pinning as the nucleation field reduces at higher Ar^+ ion energies. Within this model, the perpendicular VSM data demonstrate that the nucleation field (and hence coercivity) scales with anisotropy.

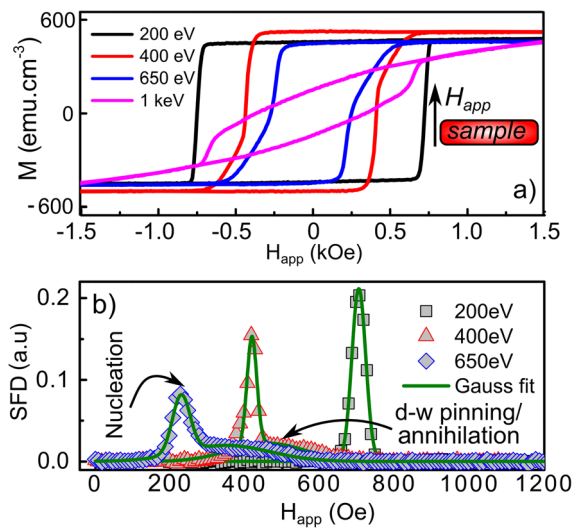

FIG. 5. [(a) and (b)] VSM analysis of the $[Co/Pd]_8$ multilayer, showing the hysteresis loops measured with the external field applied perpendicular to the sample plane (easy-axis). (a) shows the easy-axis hysteresis loops and (b) shows the normalised switching field distribution for the multilayers deposited at 200 eV, 400 eV, and 650 eV.

SUMMARY AND CONCLUSIONS

In summary, we present an *in-situ* approach of controlling the anisotropy of $[Co/Pd]_8$ by varying the acceleration energy of the Ar^+ ions during deposition. XRD and TEM measurements show that the saturation magnetization, crystallographic quality, and grain size remain constant within the uncertainty of the measurements for an Ar^+ energy range of 200 eV–1 keV. XRR data demonstrate that the interface width broadens with increasing Ar^+ energy, indicating that the interface quality is diminished; consequently, the interface anisotropy is also reduced due to the reduced symmetry breaking at the Co/Pd interface. This method allows simple and accurate control of the PMA, in principle, over single bilayer repeats not available by conventional approaches. Changing the Ar^+ ion energy within a single deposition sequence, leads to the possibility of constructing different anisotropy phases for exchange-spring type structures whilst maintaining a constant microstructure.

ACKNOWLEDGMENTS

The authors would like to thank Dr. Chris Morrison for helpful discussions and support during the course of this work. The support of the UK EPSRC through Grant No. EP/G032440/1 is gratefully acknowledged.

[1]P. F. Carcia, A. D. Meinhaldt, and A. Suna, Appl. Phys. Lett. **47**(2), 178 (1985).
[2]T. N. A. Nguyen, Y. Fang, V. Fallahi, N. Benatmane, S. M. Mohseni, R. K. Dumas, and J. Akerman, Appl. Phys. Lett. **98**(17), 172502 (2011).
[3]J. C. Slonczewski, J. Magn. Magn. Mater. **159**(1–2), L1 (1996).
[4]O. Hellwig, T. Hauet, T. Thomson, E. Dobisz, J. D. Risner-Jamtgaard, D. Yaney, B. D. Terris, and E. E. Fullerton, Appl. Phys. Lett. **95**(23), 232505 (2009).
[5]R. Sbiaa, Z. Bilin, M. Ranjbar, H. K. Tan, S. J. Wong, S. N. Piramanayagam, and T. C. Chong, J. Appl. Phys. **107**(10), 103901 (2010).
[6]J. M. Shaw, H. T. Nembach, T. J. Silva, S. E. Russek, R. Geiss, C. Jones, N. Clark, T. Leo, and D. J. Smith, Phys. Rev. B **80**(18), 184419 (2009).
[7]A. G. Roy, D. E. Laughlin, T. J. Klemmer, K. Howard, S. Khizroev, and D. Litvinov, J. Appl. Phys. **89**(11), 7531 (2001).
[8]Q. Meng, P. deHaan, W. P. vanDrent, J. C. Lodder, and T. J. A. Popma, IEEE Trans. Magn. **32**(5), 4064 (1996).
[9]T. Suzuki, H. Notarys, D. C. Dobbertin, C. J. Lin, D. Weller, D. C. Miller, and G. Gorman, IEEE Trans. Magn. **28**(5), 2754 (1992).
[10]T. Hauet, O. Hellwig, S. H. Park, C. Beigne, E. Dobisz, B. D. Terris, and D. Ravelosona, Appl. Phys. Lett. **98**(17), 172506 (2011).
[11]A. Maziewski, P. Mazalski, Z. Kurant, M. O. Liedke, J. McCord, J. Fassbender, J. Ferre, A. Mougin, A. Wawro, L. T. Baczewski, A. Rogalev, F. Wilhelm, and T. Gemming, Phys. Rev. B **85**(5), 054427 (2012).
[12]M. S. Pierce, J. E. Davies, J. J. Turner, K. Chesnel, E. E. Fullerton, J. Nam, R. Hailstone, S. D. Kevan, J. B. Kortright, K. Liu, L. B. Sorensen, B. R. York, and O. Hellwig, Phys. Rev. B **87**(18), 184428 (2013).
[13]M. Vopsaroiu, M. J. Thwaites, G. V. Fernandez, S. Lepadatu, and K. O'Grady, J. Optoelectron. Adv. Mater. **7**(5), 2713 (2005).
[14]M. Vopsaroiu, G. V. Fernandez, M. J. Thwaites, J. Anguita, P. J. Grundy, and K. O'Grady, J. Phys. D: Appl. Phys. **38**(3), 490 (2005).
[15]T. Thomson, B. Lengsfield, H. Do, and B. D. Terris, J. Appl. Phys. **103**(7), 07F548 (2008).
[16]C. Chappert and P. Bruno, J. Appl. Phys. **64**(10), 5736 (1988).
[17]P. Bruno and J. P. Renard, Appl. Phys. A: Mater. Sci. Process. **49**(5), 499 (1989).
[18]P. Chowdhury, P. D. Kulkarni, M. Krishnan, H. C. Barshilia, A. Sagdeo, S. K. Rai, G. S. Lodha, and D. V. S. Rao, J. Appl. Phys. **112**(2), 023912 (2012).
[19]J. Shirokoff and J. Courtenay Lewis, AIP Conf. Proc. **1290**(1), 274 (2010).
[20]U. Holzwarth and N. Gibson, Nat. Nanotechnol. **6**(9), 534 (2011).
[21]M. Wormington, I. Pape, T. P. A. Hase, B. K. Tanner, and D. K. Bowen, Philos. Mag. Lett. **74**(3), 211 (1996).

[22]L. G. Parratt, Phys. Rev. **95**(2), 359 (1954).
[23]A. S. Rozatian, C. H. Marrows, T. P. Hase, and B. K. Tanner, J. Phys.: Condens. Matter **17**(25), 3759 (2005).
[24]M. F. Doerner, K. Tang, T. Arnoldussen, H. Zeng, M. F. Toney, and D. Weller, IEEE Trans. Magn. **36**(1), 43 (2000).
[25]B. N. Engel, C. D. England, R. A. Vanleeuwen, M. H. Wiedmann, and C. M. Falco, Phys. Rev. Lett. **67**(14), 1910 (1991).
[26]T. Thomson, K. OGrady, and G. Bayreuther, J. Phys. D: Appl. Phys. **30**(11), 1577 (1997).
[27]M. Mansuripur, J. Appl. Phys. **63**(12), 5809 (1988).